

Available online at www.sciencedirect.com

jmr&t
Journal of Materials Research and Technology
www.jmrt.com.br



Original Article

Fabrication and characterization of PEBA fibers by melt and solution electrospinning

Zahid Sarwar, Edvinas Krugly, Paulius Pavelas Danilovas, Darius Ciuzas, Violeta Kauneliene, Dainius Martuzevicius*

Kaunas University of Technology, Faculty of Chemical Technology, Radvilenu pl. 19, Kaunas, Lithuania

ARTICLE INFO

Article history:

Received 6 June 2019

Accepted 1 October 2019

Available online xxx

Keywords:

PEBA

Melt electrospinning

Solution electrospinning

Hydrophobic membranes

ABSTRACT

Poly(ether-block-amide), often abbreviated as PEBA, is a novel polymer which is a combination of polyamide and poly ether group. The present study aimed at the fabrication of PEBA fibers by both melt and solution electrospinning. The effects of process parameters of both electrospinning techniques on fiber diameters and morphology were researched. The obtained fiber substrates were characterized for their morphology, changes in chemical composition, thermal properties, crystallinity, and hydrophobicity. Optimum results (as minimum average fiber diameter of $1.92 \pm 3.31 \mu\text{m}$) in case of melt electrospinning were obtained at tip-to-collector distance (TTCD) of 60 mm, voltage 20.0 kV, collector speed 55 rpm, and melt temperature 270°C , whereas in case of solution electrospinning TTCD of 200 mm distance and voltage of 20 kV yielded the lowest average fiber diameter of $0.37 \pm 0.34 \mu\text{m}$.

© 2019 The Authors. Published by Elsevier B.V. This is an open access article under the CC BY-NC-ND license (<http://creativecommons.org/licenses/by-nc-nd/4.0/>).

1. Introduction

PEBA is an emerging elastomer which has many versatile applications. It is a copolymer of polyamide and polyether segments [1,2]. Polyamide is a hard hydrophilic segment that is responsible for higher mechanical strength. On the other side polyether is soft hydrophobic part that gives flexibility [3–5]. Thus, it offers a balanced combination of mechanical strength, breathability, flexibility, chemical resistance, and ease of processing. Therefore, it can be applied in many fields, such as medical materials, sports market, daily life, environmental, etc. [5–7]. Specific applications of PEBA extend to separation of organic compounds [8–10] and gases [11–15], recovery of

alcohols from aqueous streams [16,17], and storing of food materials in modified atmosphere [18].

The applications taking advantage on the affinity of PEBA for certain compounds are of a specific interest in chemical engineering. Sridhar et al. [19] synthesized and characterized membranes of PEBA loaded with activated carbon for the permeability of carbon dioxide and methane gas. Sole et al. [4] developed non porous modified membranes of PEBA by using mercaptoethanol for different biomedical applications. Thanakkasaranee et al. [2] reported preparation of composite membrane of PEBA and poly ethylene glycol using solution casting technique for temperature dependent permeability of gases. Cheshomi et al. [6] fabricated thin film composite membranes for waste water treatment by coating polysulfone and polyethersulfone (PSf-PES) membrane with PEBA and using TiO_2 nanoparticles to modify the membrane.

* Corresponding author.

E-mail: daimart@ktu.lt (D. Martuzevicius).

<https://doi.org/10.1016/j.jmrt.2019.10.001>

2238-7854/© 2019 The Authors. Published by Elsevier B.V. This is an open access article under the CC BY-NC-ND license (<http://creativecommons.org/licenses/by-nc-nd/4.0/>).

While above studies report PEBA applications in the form of coated membranes, there are very few attempts to produce fibrous membranes. High surface area to volume ratio, easy process for various functionalities, mechanical strength, high speed & low cost, large porosity, and control of fiber diameter are the some major advantages over the traditional coated membranes [20–25].

Some of the most popular techniques to produce polymer fibers includes electrospinning. It is a versatile technique which is abundantly used for the production of fibers from micrometer to nanometric scale [26]. The key feature of electrospun fiber is high aspect ratio [27] that made it suitable for many potential applications in various fields such as tissue engineering, drug delivery, biomedical, textiles, filtration, sensors, catalysis, electronic devices, energy storage, and environmental applications [28–33].

The stretching of polymer cone or jet through a small nozzle with the help of electrostatic force for the generation of fiber is known as electrospinning [34,35]. Electrospinning gained rapid attention since its start from 1887 [36]. The process of electrospinning is relatively simple in which a syringe with capillary or needle, feed pump, high supply voltage source and collector are used to produce fibers. One terminal of voltage supply is attached with syringe and other is with collector. The polymer is forced through the nozzle due to the electrostatic force of repulsion of similar charges and charged species accumulate at the tip of nozzle. When this repulsion force dominates the surface tension, these charged species came out from the nozzle in the form of conical shape that is called Taylor cone [34]. The Taylor cone is elongated due the attractive force of opposite charged collector and solidify on collector in the form of fiber [37,38]. A variety of materials including polymers, ceramics, and composites can be used in electrospinning for the fabrication of fine fibers [39]. By using this technique, hollow and solid interior structures of fibers can also be developed [40].

Electrospinning is categorized into two types based on polymer state used for the formation of fiber, namely melt and solution electrospinning [41]. Melt electrospinning is also

known as solvent free electrospinning [42]. Toxicity, selectivity, environmental concerns, cost of solvents, and low production are the some major drawbacks of solution electrospinning [43,44]. The absence of solvents and its residues made melt electrospinning a safer, reliable, and greener method for the production of fibers for various applications [45] but larger diameter, complex apparatus and deficiency of suitable materials are the few drawbacks of it [46]. In melt electrospinning polymer is directly heated for the formation of fibers. The produced fibers have fewer defects and better physio mechanical properties besides higher yield [47,41].

Only one study to produce PEBA fibers by solution electrospinning was reported by Liang et al. [48]. Here PEBA was dissolved in isopropanol along with silver nanoparticles of diameter 200 nm to impart antimicrobial functionality. The diameter of resultant fibers was in micrometer range. Antibacterial results indicate that very low content of silver nanoparticles (0.15%) in PEBA fibers show excellent inhibition rate (>99.9%) against *E. coli* and *S. aureus*. Buivydiene et al. recently reported applications of melt electrospun PEBA for air filtration, however, due to issues in polymer feeding, obtained morphologies were less consistent, compared to polyamide [49], allowing for the further optimization of the spinning process.

This research presents an attempt to produce PEBA fibres by melt and solution electrospinning. Effects of process parameters such as applied voltage, tip to collector distance, melting temperature, feed rate, and collector speed on fiber morphology were investigated. The obtained fibrous mats were tested for thermal stability and changes in chemical composition.

2. Experimental

2.1. Materials

Poly(ether-block-amide) in the form of pellets was obtained from Arkema Group, France (product No Pebax 3533SP-01).

Table 1 – Design of Experiment of melt electrospinning.

Sample code	Tip-to-collector distance(mm)	Voltage (kV)	Collector speed, rpm	Temperature, °C
M1	20	10	10	300
M2	20	10	100	300
M3	20	30	100	300
M4	20	30	10	300
M5	20	30	10	240
M6	20	30	100	240
M7	20	10	100	240
M8	20	10	10	240
M9	60	20	55	270
M10	100	10	10	240
M11	100	10	100	240
M12	100	30	10	240
M13	100	30	100	240
M14	100	30	10	300
M15	100	30	100	300
M16	100	10	100	300
M17	100	10	10	300

This grade of Pebax has been selected due to its relatively high melt flow rate among the product line.

Butanol (71-36-3) and acetic acid (glacial) were purchased from Merck KGaA (Germany) and used it as received without further purification.

2.2. Preparation of filament for melt electrospinning

The pellets of PEBA were converted into filament form by using a filament extruder, which included steps of grinding, melting, extruding, cooling in cold water bath, and stretching in a roller system. This filament (diameter 1.5 mm) was the input material for melt electrospinning. The viscosity of the melt of such filament ranged from 706 Pa·s at 300 ° to 792 Pa·s at 240 °C.

2.3. Preparation of solution

The solution for electrospinning has been prepared by dissolving pellets in either glacial acetic acid or butanol. A homogenized solution of 15% w/v was prepared at 60 °C with magnetic stirring at 250 rpm for 5 h. The viscosity of solution was 17.9 Pa·s in case of butanol and 12.3 Pa·s in case of acetic acid.

2.4. Electrospinning apparatus and process

Electrospinning setups used in this study were developed in KTU and reported by Buivydiene et al. [49] and Matulevicius et al. [50].

Filament of PEBA was fed to the melt electrospinning machine by using a nozzle of 0.4 mm with a feed rate of 5 mm/min.

Solution was fed into solvent electrospinning machine by using a needle of 21 G, flow rate of 3 ml/h and collector speed of 15 rpm. The process of electrospinning was carried out in

Table 2 – Design of experiment of solution electrospinning.

Sample code	Tip-to-collector Distance (mm)	Voltage (kV)
Solvent acetic acid		
SA1	100	12
SA2	100	20
SA3	200	20
SA4	200	12
SA5	150	16
SA6	150	16
SA7	150	16
Solvent Butanol		
SB1	100	12
SB2	100	20
SB3	200	20
SB4	200	12
SB5	150	16
SB6	150	16
SB7	150	16

a closed chamber at the temperature of 22 °C and relative humidity of 40%.

2.5. Design of experiment and data analysis

The experiment was conducted following a full factorial design (MODDE 10, Umetrics, Sweden) as shown in Tables 1 and 2. Fiber morphology and characteristics mainly depend upon the process parameters [57]. Thus, experimental variables including voltage, tip-to-collector distance, temperature, and collector speed were varied in order to research their effects to the fiber morphology (represented as a mean fiber diameter).

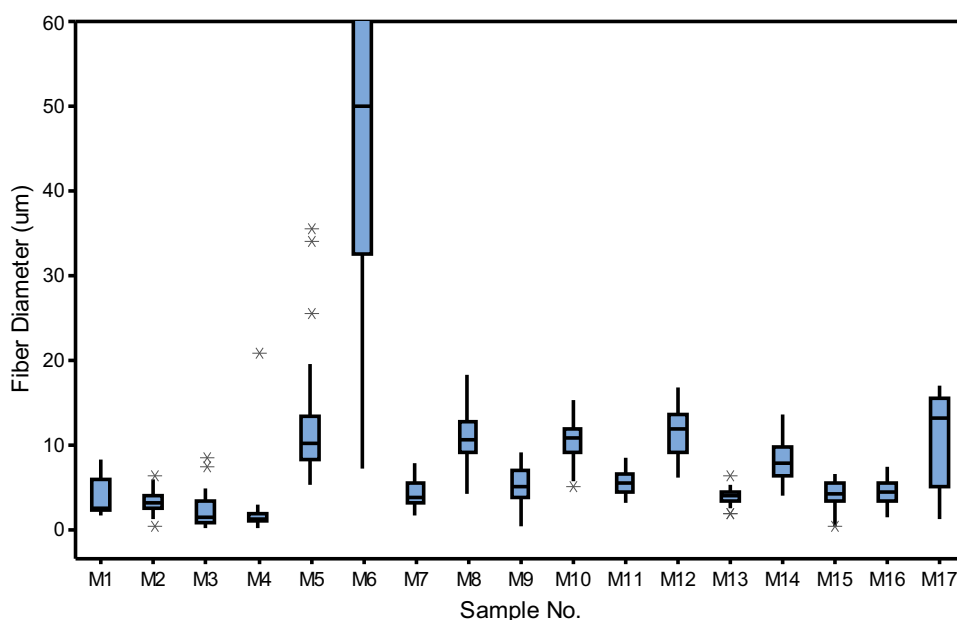


Fig. 1 – Fiber diameter distribution of melt electro spun fibers.

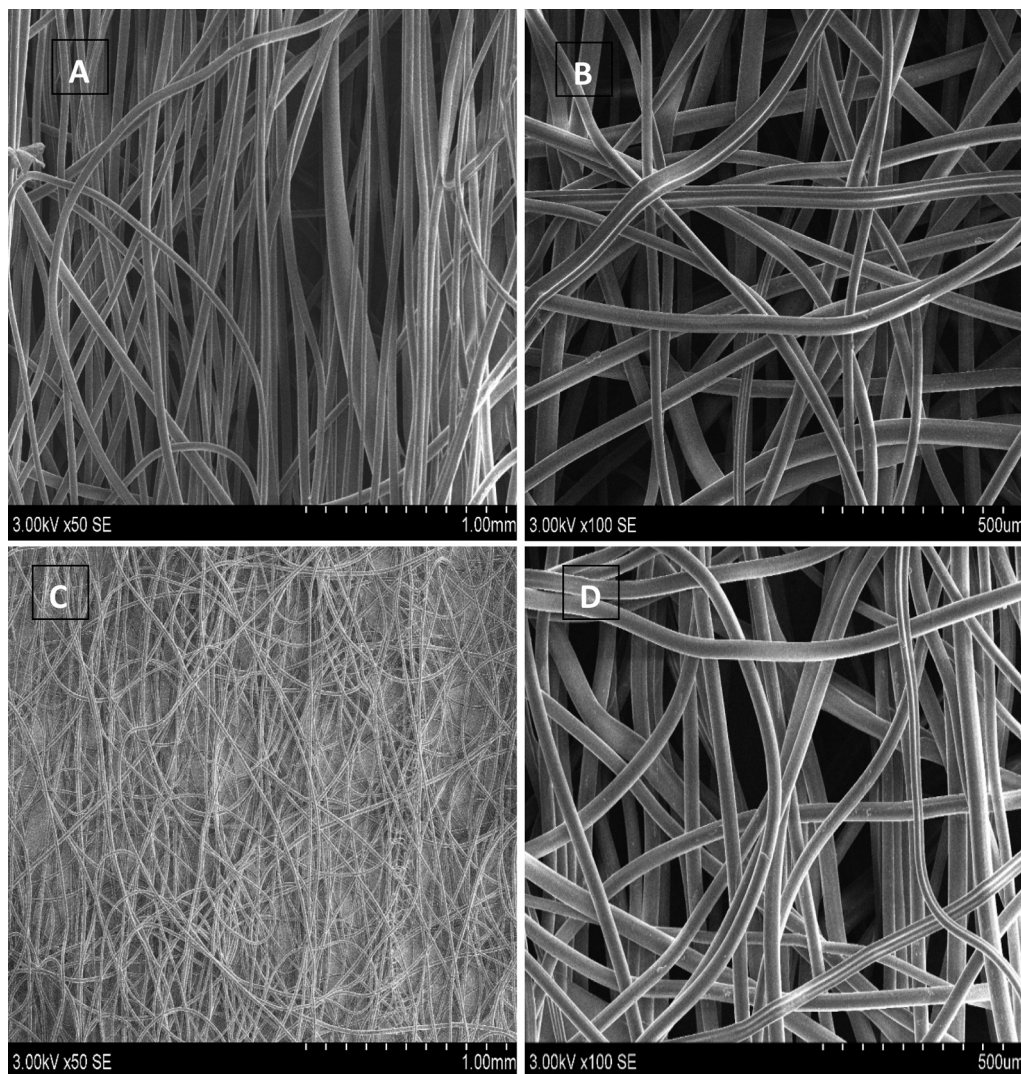


Fig. 2 – SEM images of melt electrospun samples: M4 (TTCD = 20 mm, U = 30 kV, S = 10 rpm, T = 300 °C) and M13 (TTCD = 100 mm, U = 30 kV, S = 100 rpm, T = 240 °C) at magnification of × 50 (A and C), and × 100 (B and D), respectively.

2.6. Characterization

The morphology of electrospun samples was observed by scanning electron microscopy (EVO MA10, Carl Zeiss, Germany). Image J (NIH, USA) software was used for the calculation of diameter of fibers from SEM images. 50 readings for each sample were taken and then average diameters were calculated.

Thermal stability of the produced fibers was analyzed by the thermogravimetric analysis (TGA), using by the TG analyzer (TGA 400, Perkin Elmer, USA) under nitrogen atmosphere. The temperature range is between 0 and 700 °C with a heating rate of 10 °C.min⁻¹.

The chemical composition (polymer functional groups) of the fibers (melt & solution) were characterized by infrared spectrometer (Spectrum, Perkin Elmer, USA), within the wavelength ranging from 4000–500cm⁻¹.

The crystallinity of electrospun fibers was assessed by XRD analysis (D8 Advance, Bruker-AXS, Germany) with Cu-Kα1

source. The analysis was conducted at a room temperature by scanning speed 6°/min from 5° to 90° (2θ).

The wetting behavior of electro spun fibers was evaluated by contact angle, measured with the optical tensiometer (Theta Lite, Biolin Scientific, UK). A 5 μL water droplet of deionized water was pipetted and contact angle was measured according to sessile method. This procedure was repeated at three different places for each sample and average (arithmetic mean) was taken from these results.

3. Results and discussion

3.1. Morphology of melt electro spun fibers

The obtained fibrous mats displayed a relatively large variation in fiber diameters, ranging from 1.92 to 61.70 μm (Fig. 1). The majority of diameters of the samples ranged from 1 to 10–15 μm. Generally, fiber diameter distributions were narrow,

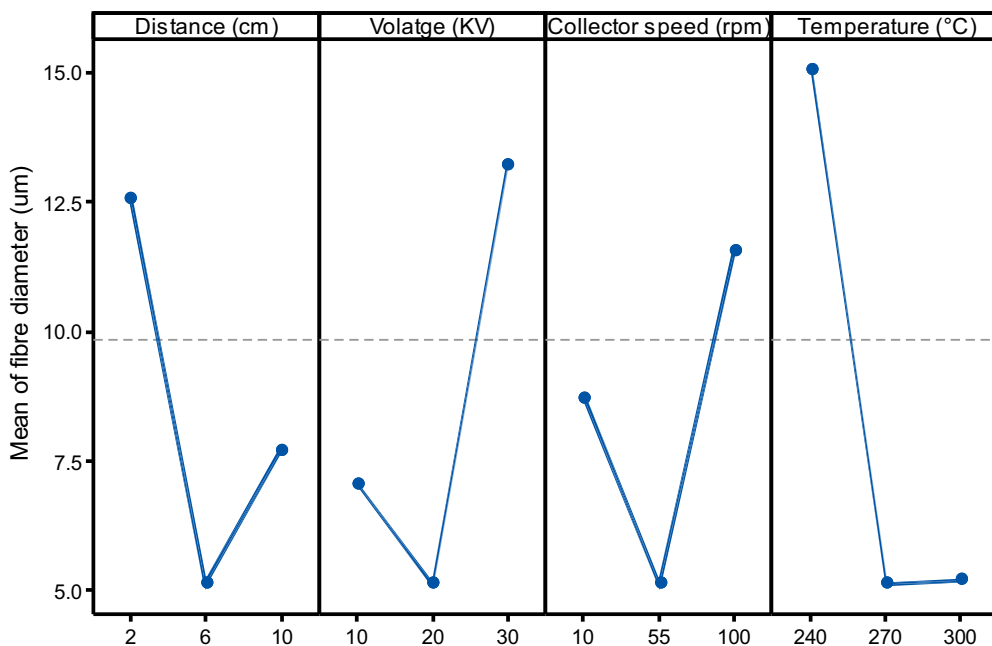


Fig. 3 – Effect of Process parameters on fiber diameter melt electro spun fibers.

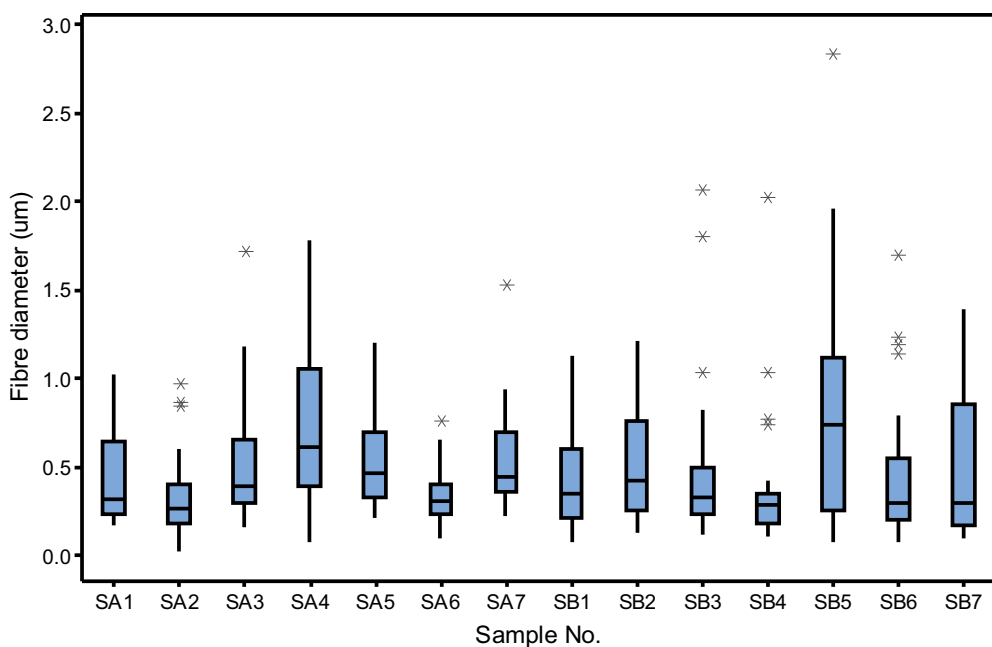


Fig. 4 – Fiber diameter distributions of solution electro spun fibers.

with the interquartile range spanning between 2 and 7 μm . The smallest fiber diameter with low dispersion has been featured in sample M4 (Fig. 2a and b), obtained at conditions of high voltage (30 kV), small TTCD (20 mm), high heating temperature (300 $^{\circ}\text{C}$) and slow rotation of collector drum (20 rpm). Specific cases were noted in samples M6 and M17, where both fiber average diameter and the dispersion were higher. M6 was a combination of low temperature (240 $^{\circ}\text{C}$), and high voltage (30 kV), which resulted in poor spinning conditions and large randomly oriented fibers. On the contrary, most samples were featuring a core of highly oriented larger fibers,

interlinked with smaller whipped ones. Similar morphology has been obtained in recent study [49], where major part of obtained samples were referred to as “parallel/disperse/thick”. Such formation has been reported to occur under low-voltage conditions and a high polymer feed rate, suggesting that in cases of overly high polymer viscosity, the electric field is not capable of initiating sufficient formation of fiber jets or whipping, thereby resulting in a process of simple drawing of the melt as opposed to electrospinning. Interestingly, we did not observe ribbon like structure, previously reported at medium or large nozzle tip diameters (0.4–0.5 mm) and high feed rate

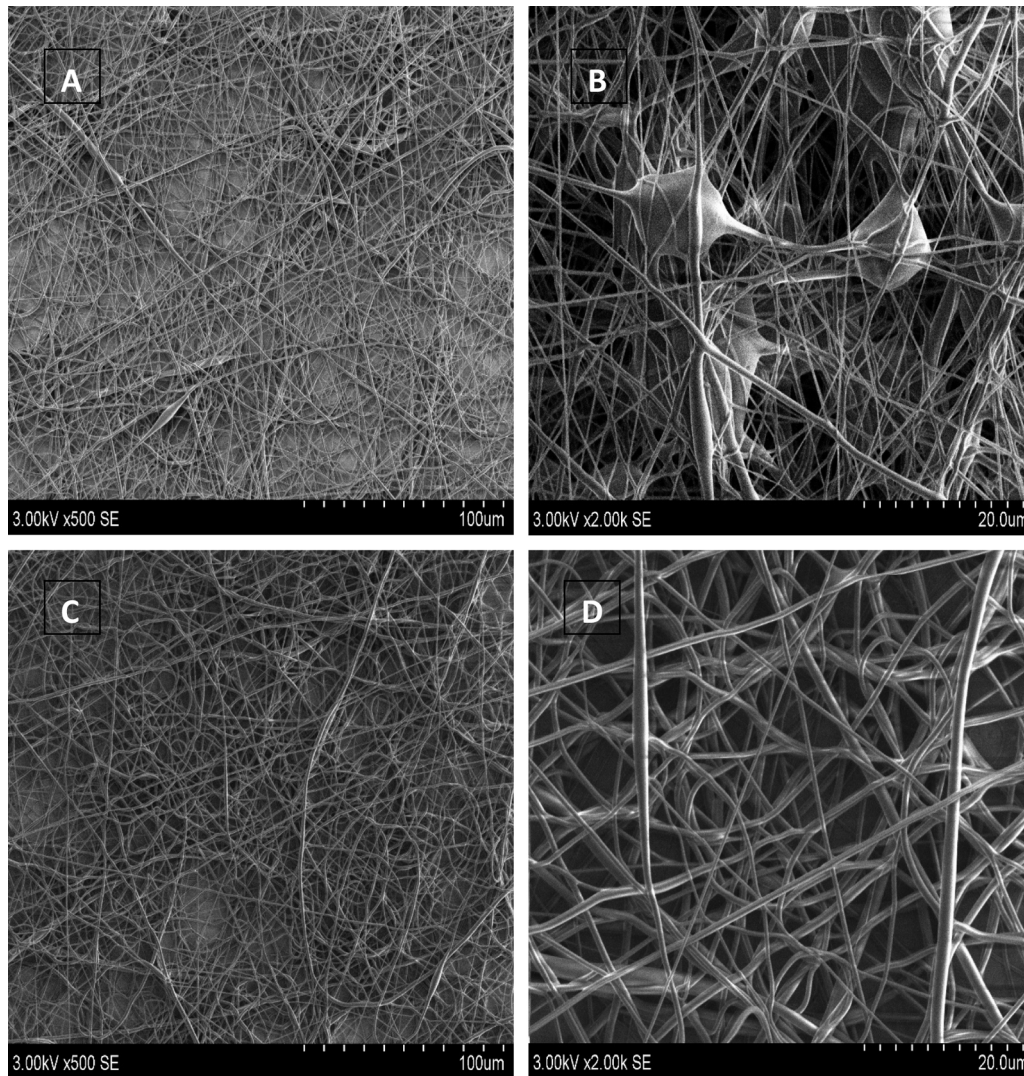


Fig. 5 – SEM images of solution electrospun mat sample: SA2 (TTCD = 100 mm, U = 20 kV and SB4 (TTCD = 200 mm, U = 12 kV at magnification of $\times 100$ (A and C), and $\times 20$ (B and D), respectively.

(20 mm/min). But generally, we were able to obtain fibers of smaller diameter, having majority at below $10\ \mu\text{m}$, as opposed to those reported by Buivydiene et al., 2019 in the range of $10\text{--}40\ \mu\text{m}$.

Effects of process parameters on the mean fiber diameter are shown in Fig. 3. It can be observed that as the collector distance increased from 20 to 60 mm, the resultant fiber diameter decreased from 12.5 to $5\ \mu\text{m}$. It is potentially due to the fact that at larger collector distance, the jet of polymer has enough time for thinning to reach the collector. The further increase of the distance to 100 mm resulted in the increase of fiber diameter to $7.5\ \mu\text{m}$. The further increase in distance reduced the electrostatic field and jet solidified before reaching the collector, as suggested by [51], who observed similar phenomenon by electrospinning low-density polyethylene.

The increasing voltage from 10 to 20 kV resulted in the decreasing fiber diameter from 7 to $5\ \mu\text{m}$, due to more intensive stretching of a fiber by an oppositely charged collector [52]. However, the further increase in voltage to 30 kV caused

fiber diameter to increase to the average of $13\ \mu\text{m}$. The possible reason is that polymer jet is solidifies in the way before reaching the collector due to less time available for cooling under extensive applied voltage. Similar observation has been reported during melt electrospinning of polypropylene, where fiber diameter increased from 8 to $10\ \mu\text{m}$, following the increase of the voltage from 70 to 90 kV [53].

Increase in collector speed to a specific value decreased the fiber diameter. Further increase in the collector speed from that specific value increase the diameter of fiber. These results agree with those reported by [54]. Increase in temperature from 240 to $270\ ^\circ\text{C}$ decreased the diameter of fiber from ~ 15 to $\sim 5\ \mu\text{m}$. This is because increase in temperature decreased the viscosity of polymer and jet of polymer is easily stretched by electrical force and it became thin. When temperature is further increased to $300\ ^\circ\text{C}$, the diameter of fiber is increased to $5.50\ \mu\text{m}$. This is may be due to very low viscosity of polymer at this temperature that increase the falling speed of jet and ultimately higher feed rate that generate beaded fibers [55].

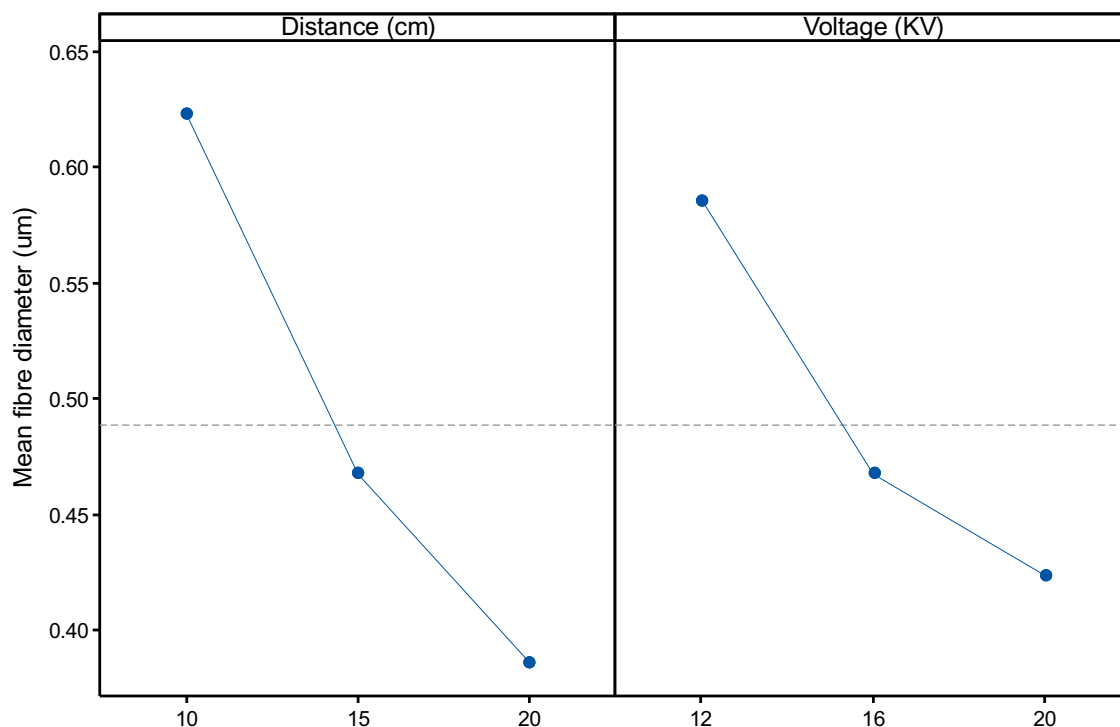


Fig. 6 – Effect of process parameters (tip-to-collector distance and voltage) on fiber diameter for solution electro spun fibers.

3.2. Morphology of solution electrospun fibers

As expected, the solution electrospinning produced fiber diameter by an order of magnitude lower compared to melt electrospinning, with majority of fibers falling within 0.2–1 µm. The dispersion of fiber diameters was relatively low, with interquartile range varying within 0.5–0.8 µm. The smallest average diameter (0.37 ± 0.34 µm) has been obtained with the sample SB4 (TTCD = 200 mm, V = 12 kV), while the largest (0.78 ± 1.25 µm) with sample SB5 (TTCD = 150, V = 16 kV) (Fig. 4).

The solvent selection (acetic acid vs. butanol) did not significantly affect fiber diameter ($p < 0.05$ based on Mann–Whitney U test). At the same time, the selection of solvent for electrospinning of PEBA is critical due to its chemical resistant nature. Butanol has proved as good choice as a solvent producing smooth and uniform fibers, but solution of PEBA in butanol tends becoming very viscous and blocking the needle of syringe. The use of acetic acid as a solvent helped overcoming the problem of needle blockage due to being of lower viscosity at the same concentration of PEBA but resulted in the formation of beaded fibers (Fig. 5). Yener et al. explored this phenomenon with polyvinyl butyral and came to conclusion that lower conductivity of acetic acid as opposed to butanol causes the formation of beads [56].

Effects of tip to collector distance and voltage on the mean fiber diameter are presented in Fig. 6. Both parameters had an reverse effect to the fiber diameter. As the collector distance increased from 100 to 200 mm, the resultant fiber diameter decreased from 0.62 to 0.39 µm. At a larger TTCD, the jet of polymer has enough time for the evaporation of solvent and thus reaching collector at a low diameter. This is a well established phenomenon in solution electrospinning [57].

The effects of increasing voltage to the decreasing fiber diameter has been also well researched. Charge repulsion within the polymer jet has been indicated as the main principle [58]. In our study, increasing the voltage from 12 to 20 kV resulted in the fiber diameter decrease from 0.59 to 0.42 µm, respectively.

3.3. Thermal stability

The PEBA material has a one-step thermal degradation pattern (Fig. 7). The degradation starts at 300 °C and ends at 480 °C. Similar thermogram pattern was reported previously [59]. PEBA is known by its relatively high thermal stability which is attributed to a random chain scission mechanism in the structure [60,61]. At the same time, electrospun fibrous material has not changed the core properties of raw polymer. The melt electrospun sample provided a sharper (although not significantly) degradation curve (Tables 1 and 2).

3.4. Chemical composition

Fig. 8 displays FTIR spectra, which indicate characteristic peaks for PEBA polymer. The peak at 3300 cm^{-1} occurs due to N–H stretching, peaks at 2923 and 2850 cm^{-1} correspond to the asymmetric and symmetric stretching of the C–H bond in amide segment. The peak at 1736 cm^{-1} corresponds to the ester carbonyl group that bond the polyamide and polyether segments together, whereas peak at 1637 cm^{-1} indicates the amide carbonyl group. Intensive peaks at 1372 and 1108 cm^{-1} represents the C–H bending and stretching vibration in ether group. Similar spectra have been reported by [62,63]. Processing of raw material by melt and solution electrospinning does

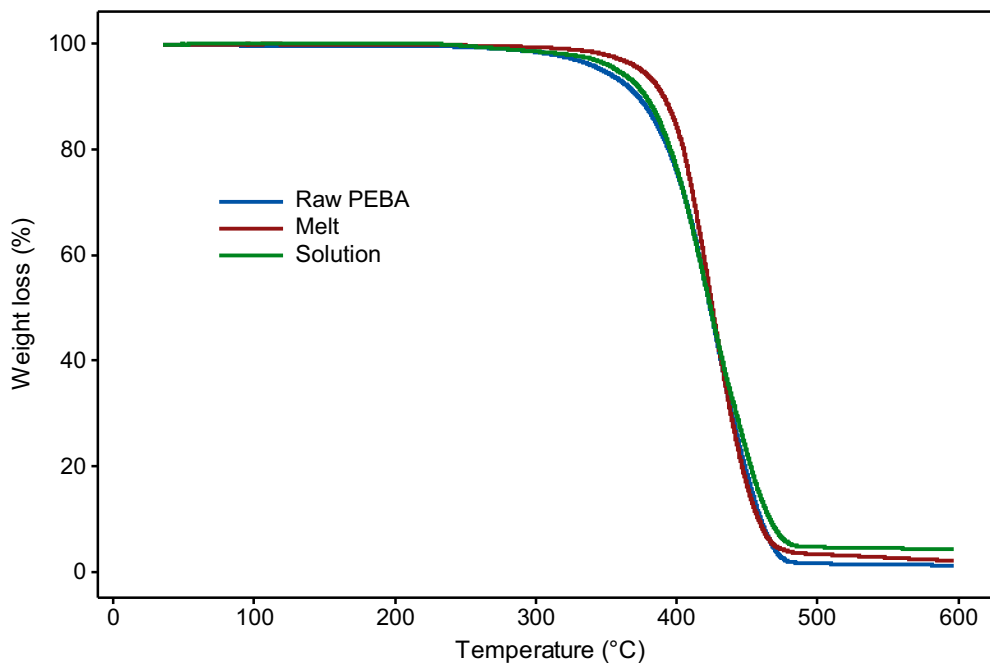


Fig. 7 – Thermogram of raw PEBA material, melt and solution electrospun fibers.

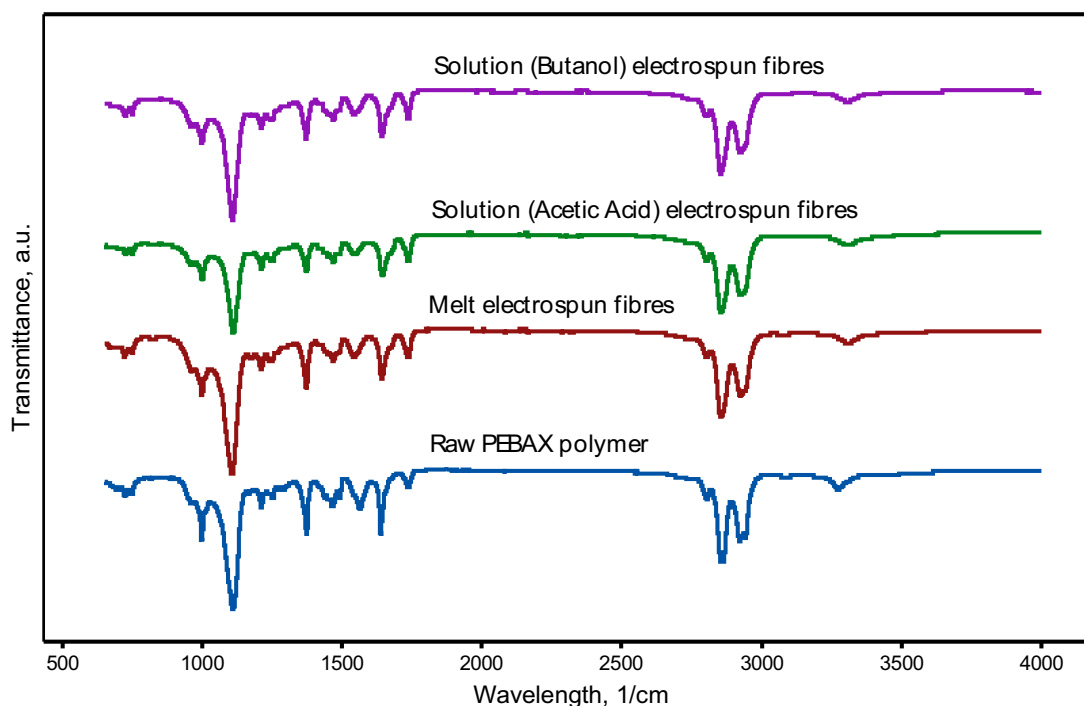


Fig. 8 – FTIR spectra of raw PEBA, melt & solution electrospun fibers.

not indicate any changes in chemical structure, confirming that these techniques are suitable for production of PEBA fibers without losing chemical properties (Figs. 9 and 10).

3.5. Wetting properties

The produced fibers were highly hydrophobic, with the measured contact angle in the range between 105 and 130 degrees (Fig 9). The contact angle increased with the decreasing

diameter of fibers. The relationship was log linear, with the regression model of $CA_{\text{melt}} = 119.2 - 18.9 \cdot \log(d_f)$, $R^2 = 0.86$ and $CA_{\text{solution}} = 120.4 - 10.3 \cdot \log(d_f)$, $R^2 = 0.81$. This opposite relationship is expected, owing to the fact that when diameter of fiber is reduced, the orientation of molecular chains and degree of crystallinity is increased [64]. The structure of higher crystallinity results in the decreased water absorbency, thus increasing the contact angle. Similar results were reported previously by [65] and [66] who observed this with solution

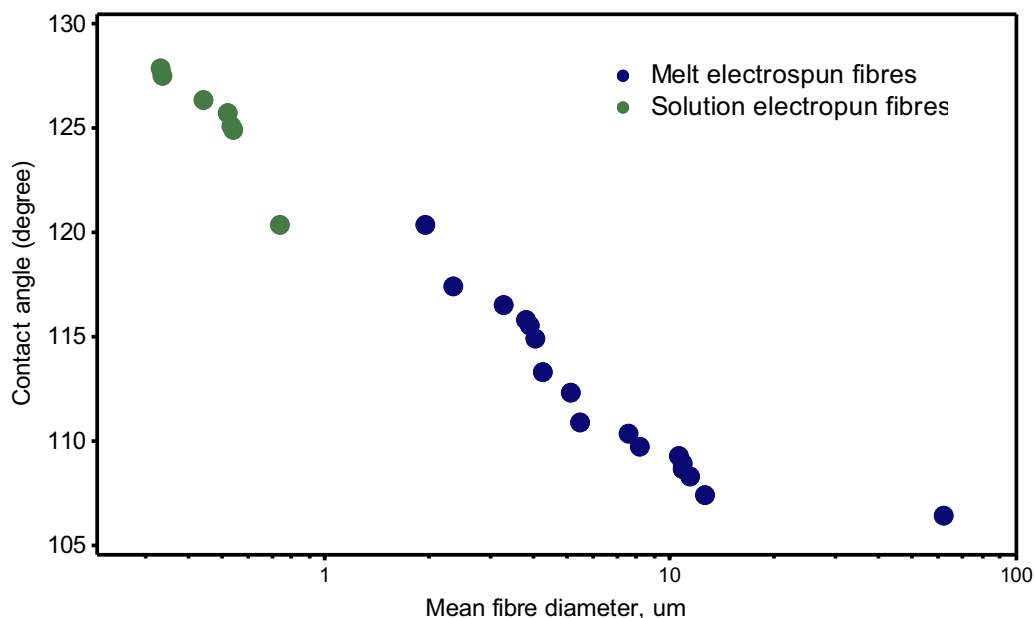


Fig. 9 – Contact angle of melt and solution electrospun fibers.

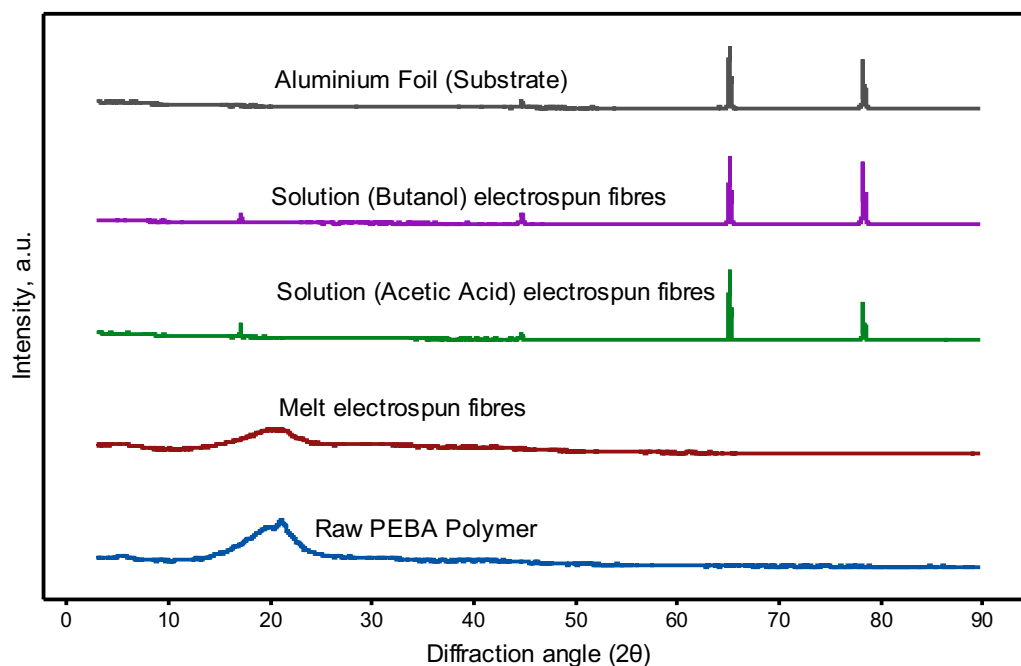


Fig. 10 – X-Ray diffraction patterns for raw PEBA, melt electrospun fibres, and solution electrospun fibres on aluminum substrate.

spun polycaprolactone, although the decrease in contact angle with the increase of fiber diameter has not been so sharp as compared to our study. Electrospun membranes of polyvinylidene fluoride-co-hexafluoropropylene (PCH) reached CA of 119° [67]. Electrospinning also results in porous and relatively rough surfaces, thus increasing the contact angle, owing to the trapped air channels in the porous membrane with heterogeneous surface [68].

Combining natural hydrophobic properties of PEBA and the structural composition of electrospun membranes, a further

exploration of these applications should be sought for separation processes (oil/water, organic mixtures, gas/liquid).

3.6. Crystallinity

Raw polymer and melt electrospun fibers show diffraction peak at $2\theta = 20^\circ$ (Fig. 10), which is similar to previous studies with PEBA as substrate for electrospinning [48] or membranes [59]. After solution electrospinning the peak is shifted at $2\theta = 17^\circ$ due to higher orientation of molecular chains in small

fiber diameter [69]. These peaks are overshadowed by the signal from aluminum foil which was used as a substrate for the collection of fibers.

4. Conclusions

Electrospun fibers of Poly(ether-block-amide) (PEBA) were successfully fabricated by using melt and solution electrospinning techniques. In both type of spinning techniques, the effect of process parameters on fiber diameter was studied and it was found that fiber diameter decreased by increasing voltage, distance, collector speed and melting temperature up to a certain limit, while further increase results in increasing fiber diameter in melt electrospinning. In solution electrospinning, the diameter of fiber is decreased by increasing voltage and distance. The fibers obtained by melt electrospinning were approx. an order of magnitude larger, compared to solution electrospinning (minimum average fiber diameters 1.92 ± 3.31 and 0.37 ± 0.34 μm , respectively). While melt electrospinning produces larger fibres, it has an advantage of not using solvents in the process thus more suitable for higher throughput production, especially when supermicrometer fibers are sufficient.

The selection of solvent for electrospinning of PEBA is important due to its chemically resistant nature. Butanol was determined as efficient solvent, resulting in smooth and uniform fibers, but causing issues in electrospinning due to increasing viscosity and blocking the needle. The use of acetic acid as a solvent can overcome this problem of needle blockage, but decreased viscosity may result in the formation of beaded fibers.

The processing of PEBA by electrospinning does not alter its thermal and chemical properties, while produced membranes have high hydrophobicity, which increases with decreasing fiber diameter. Applications of such membranes for hydrophobic packaging, separation membranes, osmotic evaporation may be sought after.

Data availability

The raw/processed data required to reproduce these findings cannot be shared at this time as the data also forms part of an ongoing study.

Conflict of interests

The authors declare that they have no known competing financial interests or personal relationships that could have appeared to influence the work reported in this paper.

Acknowledgements

Authors are grateful for Arkema Group for providing samples of PEBA for research. We would like to thank Dr. Martynas Tichonovas for the assistance in electrospinning setup preparations.

REFERENCES

- [1] Meléndez HI. Preparation and characterization of hybrid membranes based on poly(Ether-b-Amide). *Membr Mater Simulations Appl* 2016;1–154, <http://dx.doi.org/10.1007/978-3-319-45315-6>.
- [2] Thanakkasaranee S, Kim D, Seo J. Preparation and characterization of poly(ether-block-amide)/polyethylene glycol composite films with temperature- dependent permeation. *Polymers (Basel)* 2018;10, <http://dx.doi.org/10.3390/polym10020225>.
- [3] Tena A, Shishatskiy S, Filiz V. Poly(ether-amide) vs. poly(ether-imide) copolymers for post-combustion membrane separation processes. *RSC Adv* 2015;5:22310–8, <http://dx.doi.org/10.1039/c5ra01328c>.
- [4] B Sole B, Lohkna S, Chhabra PK, Prakash V, Seshadri G. Preparation of mechanically strong poly (ether block amide)/Mercaptoethanol breathable membranes for biomedical applications. *J Polym Res* 2018;25:1–12.
- [5] Metz SJ, Mulder MHV, Wessling M. Gas-permeation properties of poly(ethylene oxide) poly(butylene terephthalate) block copolymers. *Macromolecules* 2004;37:4590–7, <http://dx.doi.org/10.1021/ma049847w>.
- [6] Cheshomi N, Pakizeh M, Namvar-Mahboub M. Preparation and characterization of TiO₂/Pebax/(PSf-PES) thin film nanocomposite membrane for humic acid removal from water. *Polym Adv Technol* 2018;29:1303–12, <http://dx.doi.org/10.1002/pat.4242>.
- [7] Sutrisna PD, Hou J, Zulkifli MY, Li H, Zhang Y, Liang W, et al. Surface functionalized UiO-66/Pebax-based ultrathin composite hollow fiber gas separation membranes. *J Mater Chem A* 2018;6:918–31, <http://dx.doi.org/10.1039/c7ta07512j>.
- [8] Gu J, Zhang X, Bai Y, Yang L, Zhang C, Sun Y. ZSM-5 filled polyether block amide membranes for separating EA from aqueous solution by pervaporation. *InternationalJournalofPolymerScience* 2013;2013:10.
- [9] Sridhar S, Kalyani S, Ravikumar YVL, Muralikrishna TSVN. Performance of composite membranes of poly(ether-block-amide) for dehydration of rthylene glycol and ethanol. *Sep Sci Technol* 2010;45:322–30, <http://dx.doi.org/10.1080/01496390903409468>.
- [10] Mandal MK, Bhattacharya PK. Poly (ether-block-amide) membrane for pervaporative separation of pyridine present in low concentration in aqueous solution. *J Memb Sci* 2006;286:115–24, <http://dx.doi.org/10.1016/j.memsci.2006.09.022>.
- [11] Kok Chung C, Lai SO, Lau WJ, Thiam HS, Ismail AF, Roslan RA. Preparation, characterization, and performance evaluation of polysulfone hollow Fiber membrane with PEBA or PDMS coating for oxygen enhancement process. *Polymers (Basel)* 2018;126:1–11, <http://dx.doi.org/10.3390/polym10020126>.
- [12] Abbass Kazemi A, Gamali P, Mohammadreza Rahmani M, Pourkhalil M. Improved gas separation of PEBA-CSWCNTs mixed matrix membranes. *J Membr Sep Technol* 2017;6:55–70, <http://dx.doi.org/10.6000/1929-6037.2017.06.02.3>.
- [13] Doddy P, Hou J, Li H, Zhang Y, Chen V. Improved operational stability of Pebax-based gas separation membranes with ZIF-8: a comparative study of flat sheet and composite hollow fibre membranes. *J Memb Sci* 2017;524:266–79, <http://dx.doi.org/10.1016/j.memsci.2016.11.048>.
- [14] Volodin A, Vankelecom IFJ, Didden J, Th R. Blending PPO-based molecules with Pebax MH 1657 in membranes for gas separation. *J Appl Polym Sci* 2018;135:1–12, <http://dx.doi.org/10.1002/app.46433>.
- [15] Habibiannejad SA, Aroujalian A, Raisi A. Pebax-1657 mixed matrix membrane containing surface modified multi-walled

- carbon nanotubes for gas separation. *RSC Adv* 2016;6:79563–77, <http://dx.doi.org/10.1039/c6ra14141b>.
- [16] Le NL, Wang Y, Chung TS. Pebax/POSS mixed matrix membranes for ethanol recovery from aqueous solutions via pervaporation. *J Memb Sci* 2011;379:174–83, <http://dx.doi.org/10.1016/j.memsci.2011.05.060>.
- [17] Najafi M, Mousavi SM, Saljoughi E. Preparation and characterization of poly(Ether block amide)/graphene membrane for recovery of isopropanol from aqueous solution via pervaporation. *Polym Compos* 2018;39:2259–67, <http://dx.doi.org/10.1002/pc.24203>.
- [18] Watawala MWM, Eyer MDM, Akundi RHM, Aerere APM. Original article Biodiversity of fruit flies (Diptera, Tephritidae) in orchards in different agro-ecological zones of the Morogoro region, Tanzania. *Fruits* 2018;57:313–22, <http://dx.doi.org/10.1051/fruits>.
- [19] Sridhar S, Smitha B, Suryamurali R, Aminabhavi TM. Synthesis, characterization and gas permeability of an activated carbon-loaded PEBAX 2533 membrane. *Des Monomers Polym* 2008;11:17–27, <http://dx.doi.org/10.1163/15685508X292392>.
- [20] Wu H, Pan W, Lin D, Li H. Electrospinning of ceramic nanofibers: Fabrication, assembly and applications. *J Adv Ceram* 2012;1:2–23, <http://dx.doi.org/10.1007/s40145-012-0002-4>.
- [21] Mondal K. Recent advances in the synthesis of metal oxide nanofibers and their environmental remediation applications. *Inventions* 2017;2:1–29, <http://dx.doi.org/10.3390/inventions2020009>.
- [22] Kenry CT. Nanofiber technology: current status and emerging developments. *Prog Polym Sci* 2017;70:1–17, <http://dx.doi.org/10.1016/j.progpolymsci.2017.03.002>.
- [23] Mokhtari F, Salehi M, Zamani F, Hajiani F, Zeighami F, Latifi M. Advances in electrospinning: the production and application of nanofibres and nanofibrous structures. *Text Prog* 2016;48:119–219, <http://dx.doi.org/10.1080/00405167.2016.1201934>.
- [24] Ramesh Kumar P, Khan N, Vivekanandhan S, Satyanarayana N, Mohanty AK, Misra M. Nanofibers: effective generation by electrospinning and their applications. *J Nanosci Nanotechnol* 2012;12:1–25, <http://dx.doi.org/10.1166/jnn.2012.5111>.
- [25] Gong W, Wang X, Li Z, Gu J. A high-strength PPEK/PVDF fibrous membrane prepared by coaxial electrospinning for lithium-ion battery separator. *High Perform Polym* 2018:1–11, <http://dx.doi.org/10.1177/0954008318814154>.
- [26] Zhang X, Reagan MR, Kaplan D. Electrospun silk biomaterial scaffolds for regenerative medicine. *Adv Drug Deliv Rev* 2009;61:988–1006, <http://dx.doi.org/10.1016/j.addr.2009.07.005>.
- [27] Panda PK, Sahoo B. Synthesis and applications of electrospun nanofibers - a review. *Nanotechnology, Fundam Appl* 2013;1:399–416.
- [28] Vasita R, Katti DS. Nanofibers and their applications in tissue engineering. *Int J Nanomedicine* 2006:15–30.
- [29] Hu X, Liu S, Zhou G, Huang Y, Xie Z, Jing X. Electrospinning of polymeric nano fibers for drug delivery applications. *J Control Release* 2014;185:12–21, <http://dx.doi.org/10.1016/j.jconrel.2014.04.018>.
- [30] Witold K, Louda P, Mitura SF. Potential applications of nanofiber textile covered by carbon coatings. *J Achiev Mater Manuf Eng* 2008;27:35–8.
- [31] Podgórski A, Bałazy A, Grado L. Application of nanofibers to improve the filtration efficiency of the most penetrating aerosol particles in fibrous filters. *Chem Eng Sci* 2006;61:6804–15, <http://dx.doi.org/10.1016/j.ces.2006.07.022>.
- [32] Ouyang Z, Li J, Wang J, Li Q, Ni T, Zhang X, et al. Fabrication, characterization and sensor application of electrospun polyurethane nanofibers filled with carbon nanotubes and silver nanoparticles. *J Mater Chem B* 2013;1:2415–24, <http://dx.doi.org/10.1039/c3tb20316f>.
- [33] Thavasi V, Singh G, Ramakrishna S. Electrospun nanofibers in energy and environmental applications. *Energy Environ Sci* 2008;1:205–21, <http://dx.doi.org/10.1039/b809074m>.
- [34] King SG, Stolojan V, Silva SRP. Large area uniform electrospun polymer nanofibers by balancing of the electrostatic field. *React Funct Polym* 2018;129:89–94, <http://dx.doi.org/10.1016/j.reactfunctpolym.2017.10.017>.
- [35] Hohman MM, Shin M, Rutledge G, Brenner MP. Electrospinning and electrically forced jets. I. Stability theory. *Phys Fluids* 2001;13:2201–20, <http://dx.doi.org/10.1063/1.1384013>.
- [36] Tucker N, Stanger JJ, Staiger MP, Razzaq H, Hofman K. The history of the science and technology of electrospinning from 1600 to 1995. *J Eng Fiber Fabr* 2018;7:155892501200702, <http://dx.doi.org/10.1177/155892501200702s10>.
- [37] Garg K, Bowlin GL. Electrospinning jets and nanofibrous structures. *Biomicrofluidics* 2011;5:1–19, <http://dx.doi.org/10.1063/1.3567097>.
- [38] Sahay R, Thavasi V, Ramakrishna S. Design modifications in electrospinning setup for advanced applications. *J Nanomater* 2011;2011:1–17, <http://dx.doi.org/10.1155/2011/317673>.
- [39] Shi X, Zhou W, Ma D, Ma Q, Bridges D, Ma Y, et al. Electrospinning of nanofibers and their applications for energy devices. *J Nanomater* 2015;16:1–20.
- [40] Xue J, Xie J, Liu W, Xia Y. Electrospun nanofibers: new concepts, materials, and applications. *Acc Chem Res* 2017;50:1976–87, <http://dx.doi.org/10.1021/acs.accounts.7b00218>.
- [41] Lian H, Meng Z. Melt electrospinning vs. solution electrospinning: a comparative study of drug-loaded poly (ϵ -caprolactone) fibres. *Mater Sci Eng C* 2017;74:117–23, <http://dx.doi.org/10.1016/j.msec.2017.02.024>.
- [42] Muerza-Cascante ML, Haylock D, Hutmacher DW, Dalton PD. Melt electrospinning and its technologization in tissue engineering. *Tissue Eng Part B Rev* 2015;21:187–202, <http://dx.doi.org/10.1089/ten.teb.2014.0347>.
- [43] Xie G, Chen Z, Ramakrishna S, Liu Y. Orthogonal design preparation of phenolic fiber by melt electrospinning. *J Appl Polym Sci* 2015;132, <http://dx.doi.org/10.1002/app.42574>.
- [44] Liu Y, Deng R, Hao M, Yan H, Yang W. Orthogonal design study on factors effecting on fibers diameter of melt electrospinning. *Polym Eng Sci* 2010;50:2074–8, <http://dx.doi.org/10.1002/pen>.
- [45] Bubakir MM, Li H, Barhoum A, Yang W. Advances in melt electrospinning technique. *Handb. Nanofibers* 2017:1–32.
- [46] Li-Hua Z, Duan X-P, Yan X, Yu M, Ning X, Yong Zhao Y-ZL. Recent advances in melt electrospinning. *RSC Adv* 2016;6:53400–14, <http://dx.doi.org/10.1039/c6ra09558e>.
- [47] Morikawa Kai, Green Micah ANM. A novel approach for melt electrospinning of polymer fibers. *Procedia Manuf* 2018;26:205–8, <http://dx.doi.org/10.1016/j.promfg.2018.07.028>.
- [48] Liang S, Zhang G, Min J, Ding J, Jiang X. Synthesis and antibacterial testing of silver/poly (ether amide) composite nanofibers with ultralow silver content. *J Nanomater* 2014;4:1–10, <http://dx.doi.org/10.1155/2014/684251>.
- [49] Buivydiene D, Ciuzas D, Tichonovas M, Kliucininkas L, Martuzevicius D. Formation and characterisation of air filter material printed by melt electrospinning. *J Aerosol Sci* 2019;131:48–63, <http://dx.doi.org/10.1016/j.jaerosci.2019.03.003>.
- [50] Matulevicius J, Kliucininkas L, Prasauskas T, Buivydiene D, Martuzevicius D. The comparative study of aerosol filtration by electrospun polyamide, polyvinyl acetate, polyacrylonitrile and cellulose acetate nanofiber media. *J*

- Aerosol Sci 2016;92:27–37,
<http://dx.doi.org/10.1016/j.jaerosci.2015.10.006>.
- [51] Deng R, Liu Y, Ding Y, Xie P, Luo L, Yang W. Melt electrospinning of low-density polyethylene having a low-melt flow index. *J Appl Polym Sci* 2009;114:166–75,
<http://dx.doi.org/10.1002/app>.
- [52] Yuan X, Zhang Y, Dong C, Sheng J. Morphology of ultrafine polysulfone fibers prepared by electrospinning. *Polym Int* 2004;53:1704–10, <http://dx.doi.org/10.1002/pi.1538>.
- [53] Hao M, Liu Y, He X, Ding Y, Yang W. Factors influencing diameter of polypropylene fiber in melt electrospinning. *Adv Polym Sci Eng* 2011;221:129–34,
<http://dx.doi.org/10.4028/www.scientific.net/AMR.221.129>.
- [54] Sadat A, Hamid M, Hajiesmaeilbaigi F. Effect of electrospinning parameters on morphological properties of PVDF nanofibrous scaffolds. *Prog Biomater* 2017;6:113–23,
<http://dx.doi.org/10.1007/s40204-017-0071-0>.
- [55] Shen Y, Liu Q, Deng B, Yao P, Xia S. Experimental study and prediction of the diameter of melt-electrospinning polypropylene fiber. *Fibers Polym* 2016;17:1227–37,
<http://dx.doi.org/10.1007/s12221-016-6303-4>.
- [56] Yener F, Yalcinkaya B. Electrospinning of polyvinyl butyral in different solvents. *E-Polymers* 2013;13:229–42,
<http://dx.doi.org/10.1515/epoly-2013-0121>.
- [57] Haider A, Haider S, Kang I. A comprehensive review summarizing the effect of electrospinning parameters and potential applications of nanofibers in biomedical and biotechnology. *Arab J Chem* 2018;11:1165–88,
<http://dx.doi.org/10.1016/j.arabjc.2015.11.015>.
- [58] Haider A, Haider S, Kang I. A comprehensive review summarizing the effect of electrospinning parameters and potential applications of nanofibers in biomedical and biotechnology. *Arab J Chem* 2018;11:1165–88,
<http://dx.doi.org/10.1016/j.arabjc.2015.11.015>.
- [59] Varghese L, Issac MV, Tom RM, Abraham NM, Shamil MN. A study on pebax 3533 | SiO₂ polymer films. *J Basic Appl Eng Res* 2015;2:1818–22.
- [60] Thanak Kasaranee S, Kim D, Seo J. Preparation and characterization of Poly (ether-block-amide)/polyethylene glycol composite films with temperature - dependent permeation. *Polymers (Basel)* 2018;10:1–16,
<http://dx.doi.org/10.3390/polym10020225>.
- [61] Ghosh S, Khastgir D, Bhowmick AK, Mukunda PG. Thermal degradation and ageing of segmented polyamides. *Polym Degrad Stab* 2000;67:427–36.
- [62] Nafisi V, Hägg MB. Development of dual layer of ZIF-8/PEBAX-2533 mixed matrix membrane for CO₂ capture. *J Memb Sci* 2014;459:244–55,
<http://dx.doi.org/10.1016/j.memsci.2014.02.002>.
- [63] Esposito E, Clarizia G, Bernardo P, Carolus J, Sedláková Z, Izák P, et al. Pebax®/PAN hollow fiber membranes for CO₂/CH₄ separation. *Chem Eng Process - Process Intensif* 2015;94:53–61, <http://dx.doi.org/10.1016/j.cep.2015.03.016>.
- [64] Wong S, Baji A, Leng S. Effect of fiber diameter on tensile properties of electrospun poly(ϵ -caprolactone). *Polymer (Guildf)* 2008;49:4713–22,
<http://dx.doi.org/10.1016/j.polymer.2008.08.022>.
- [65] Ma M, Mao Y, Gupta M, Gleason KK, Rutledge GC. Superhydrophobic fabrics produced by electrospinning and chemical vapor deposition. *Macromolecules* 2005;38:9742–8,
<http://dx.doi.org/10.1021/ma0511189>.
- [66] Yohe ST, Freedman JD, Falde EJ, Colson YL, Grinstaff MW. A mechanistic study of wetting superhydrophobic porous 3D meshes. *Adv Funct Mater* 2013;23:3628–37,
<http://dx.doi.org/10.1002/adfm.201203111>.
- [67] Zhang L, Shi X, Peng X, Chen B, Kuang T. Enhanced hydrophobicity of electrospun polyvinylidene fluoride-co-hexafluoropropylene membranes by introducing modified nanosilica. In: *Annu. Tech. Conf. - ANTEC, Conf. Proc.* 2017. p. 586–90, vol. 2017- May.
- [68] Ahmad NA, Leo CP, Ahmad AL, Ramli WKW. Membranes with great hydrophobicity: a review on preparation and characterization. *Sep Purif Rev* 2015;44:109–34,
<http://dx.doi.org/10.1080/15422119.2013.848816>.
- [69] Wong SC, Baji A, Leng S. Effect of fiber diameter on tensile properties of electrospun poly(ϵ -caprolactone). *Polymer (Guildf)* 2008;49:4713–22,
<http://dx.doi.org/10.1016/j.polymer.2008.08.022>.